This article is a *Plant Cell* Advance Online Publication. The date of its first appearance online is the official date of publication. The article has been edited and the authors have corrected proofs, but minor changes could be made before the final version is published. Posting this version online reduces the time to publication by several weeks.

Mutation of *Arabidopsis SPLICEOSOMAL TIMEKEEPER LOCUS1* Causes Circadian Clock Defects[W]

Matthew A. Jones,[a,1] Brian A. Williams,[a] Jim McNicol,[b] Craig G. Simpson,[c] John W.S. Brown,[c,d] and Stacey L. Harmer[a,2]

[a] Department of Plant Biology, College of Biological Sciences, University of California, Davis, California, 95616
[b] Biomathematics and Statistics Scotland at Scottish Crop Research Institute, Invergowrie, Dundee DD2 5DA, Scotland, United Kingdom
[c] Cell and Molecular Sciences, The James Hutton Institute, Invergowrie, Dundee, Scotland, DD2 5DA, United Kingdom
[d] Division of Plant Sciences, University of Dundee at James Hutton Institute, Invergowrie, Dundee, Scotland DD2 5DA, United Kingdom

The circadian clock plays a crucial role in coordinating plant metabolic and physiological functions with predictable environmental variables, such as dusk and dawn, while also modulating responses to biotic and abiotic challenges. Much of the initial characterization of the circadian system has focused on transcriptional initiation, but it is now apparent that considerable regulation is exerted after this key regulatory step. Transcript processing, protein stability, and cofactor availability have all been reported to influence circadian rhythms in a variety of species. We used a genetic screen to identify a mutation within a putative RNA binding protein (*SPLICEOSOMAL TIMEKEEPER LOCUS1* [*STIPL1*]) that induces a long circadian period phenotype under constant conditions. STIPL1 is a homolog of the spliceosomal proteins TFP11 (*Homo sapiens*) and Ntr1p (*Saccharomyces cerevisiae*) involved in spliceosome disassembly. Analysis of general and alternative splicing using a high-resolution RT-PCR system revealed that mutation of this protein causes less efficient splicing of most but not all of the introns analyzed. In particular, the altered accumulation of circadian-associated transcripts may contribute to the observed mutant phenotype. Interestingly, mutation of a close homolog of *STIPL1*, *STIP-LIKE2*, does not cause a circadian phenotype, which suggests divergence in function between these family members. Our work highlights the importance of posttranscriptional control within the clock mechanism.

INTRODUCTION

The diurnal rhythm generated as the Earth spins on its axis has produced an evolutionary pressure to coordinate metabolic and physiological processes with regular changes in the environment (Hut and Beersma, 2011). Such coordination is achieved through the action of the circadian system, a timing mechanism consisting of interlocked feedback loops that generate a sustainable oscillation of ~24 h (Harmer, 2009). While much of the initial characterization of the circadian system focused upon transcriptional regulation, it is now apparent that considerable regulation occurs posttranscriptionally (Cibois et al., 2010; Kojima et al., 2011; Zhang et al., 2011). Transcript processing (in particular, alternative splicing [AS]), protein stability, and cofactor availability have all been reported to influence circadian rhythms in a variety of species (Nakahata et al., 2008; Filichkin et al., 2010; van Ooijen et al., 2011; James et al., 2012).

Circadian clocks appear to have evolved independently in multiple lineages but share a common organizational structure (Rosbash, 2009). In plants, the transcriptional component of the circadian system consists of multiple, interlocked negative feedback loops (reviewed in Nakamichi, 2011). During the morning, two MYB-like transcription factors, CIRCADIAN CLOCK ASSOCIATED1 (CCA1) and LATE ELONGATED HYPOCOTYL (LHY), promote expression of *PSEUDORESPONSE REGULATOR7* (*PRR7*) and *PRR9* (Farré et al., 2005), which in turn repress expression of *CCA1* and *LHY* (Farré and Kay, 2007; Nakamichi et al., 2010). In the evening, GIGANTEA (GI) and ZEITLUPE act to regulate the stability of TIMING OF CAB EXPRESSION1 (TOC1; Más et al., 2003; Kim et al., 2007). These morning and evening components are linked via the repression of *TOC1* expression by CCA1 and LHY, while TOC1 inhibits expression of *CCA1* and *LHY* (Alabadí et al., 2001; Gendron et al., 2012; Huang et al., 2012).

Advances in high-throughput sequencing techniques continue to reveal the extent of AS in plants. Indeed, a recent study revealed that >60% of intron-containing genes undergo AS (Marquez et al., 2012). AS is involved in a wide range of plant processes, including growth and development, flowering time, and responses to environmental conditions and pathogens (Ali and Reddy, 2008; Barbazuk et al., 2008). AS has also been shown to be involved in regulation of the circadian clock. Retention of intron 4 within *CCA1* is conserved between different species (Filichkin et al., 2010), and a mutation in *PROTEIN ARGININE METHYL TRANSFERASE5* (*PRMT5*) induces a longer circadian period and dramatic changes in the levels of unproductive *PRR9* AS transcripts (Hong et al., 2010; Sanchez et al., 2010). Recently, an extensive analysis of AS in core circadian clock genes has demonstrated both the widespread occurrence of AS in these

[1] Current address: School of Biological Sciences, University of Essex, Wivenhoe Park, Colchester CO4 3SQ, United Kingdom.
[2] Address correspondence to slharmer@ucdavis.edu.
The author responsible for distribution of materials integral to the findings presented in this article in accordance with the policy described in the Instructions for Authors (www.plantcell.org) is: Stacey L. Harmer (slharmer@ucdavis.edu).
[W] Online version contains Web-only data.
www.plantcell.org/cgi/doi/10.1105/tpc.112.104828

genes and the dynamic, reversible production of AS isoforms in response to changes in temperature (James et al., 2012). Such alternatively spliced isoforms may alter the pace of the clock by interfering with the function of the FS isoform (Seo et al., 2012). AS is therefore an additional mechanism involved in the operation and control of the plant circadian clock and may be important in adaptation to different conditions to which plants are exposed.

Following the initiation of transcription, precursor mRNAs (pre-mRNAs) are processed to mRNAs through pre-mRNA splicing, which removes introns and ligates exons together. Splicing is catalyzed by the spliceosome, a complex, megadalton-sized structure with multiple components (Chen and Manley, 2009; Will and Lührmann, 2011) and is a two-step process involving two ATP-independent transesterification reactions that generate a mature mRNA and a lariat intron (Staley and Guthrie, 1998). Release of the lariat intron is an essential step that is regulated by a variety of proteins, including TUFTELIN-INTERACTING PROTEIN11 (TFIP11; Tannukit et al., 2009). TFIP11 has been identified as a constituent of the spliceosome in several proteomic studies (Jurica et al., 2002; Makarov et al., 2002; Rappsilber et al., 2002; Zhou et al., 2002) and is a member of the *SEPTIN AND TUFTELIN INTERACTING PROTEIN* (*STIP*) family of genes. *STIP* genes are present in one copy in animal genomes and, at least in *Caenorhabditis elegans*, *STIP* is essential for viability (Ji et al., 2007). Here, we report the role of an *Arabidopsis thaliana* TFIP11 homolog in efficient splicing of genes that act within the plant circadian clock. *Arabidopsis* SPLICEOSOMAL TIMEKEEPER LOCUS1 (STIPL1) and its paralog, STIPL2, share homology with members of the STIP family (Ji et al., 2007), but only mutation of *STIPL1* induces a circadian defect under free-running conditions. Such data suggest a specialization of function following duplication of the ancestral gene.

RESULTS

STIPL1 Is a Member of a Conserved Protein Family

To discover new genes and alleles with a role in the plant circadian clock, we mutagenized *Arabidopsis* plants carrying a clock-regulated bioluminescent reporter, *Cold, Circadian Rhythm, and RNA Binding 2*:*Luciferase* (*CCR2*:*LUC*). Progeny were assayed in constant conditions, and mutants with altered free-running circadian rhythms were selected as previously described (Martin-Tryon et al., 2007). One such mutant was isolated on the basis of an enhanced bioluminescence, long-period phenotype (Figure 1A). We then used publicly available simple sequence length polymorphism markers to identify the locus responsible for this phenotype (Jander et al., 2002). After screening 1576 plants from an F2 mapping population, we identified a 46-kb region on chromosome 1 that cosegregated with the long-period phenotype. This region contains 15 annotated genes (see Supplemental Table 1 online). Sequencing of candidate loci led to the identification of a G-to-A transition within the gene At1g17070 that is predicted to generate a premature termination codon (PTC; Figure 1B). At1g17070 shares significant homology with *STIP* genes identified in other metazoa (Ji et al., 2007), and we therefore designated our mutant *stipl1-1*. As a lesion in *STIPL1* appeared to be responsible for the observed long-period circadian phenotype, we identified an additional T-DNA insertion line within the *STIPL1* locus from the SAIL collection (Sessions et al., 2002) and renamed this allele *stipl1-2* (Figure 1B). For both mutant alleles, *STIPL1* transcripts were readily detected but at reduced levels (Figure 1C) and likely represent unproductive, nonsense-mediated decay (NMD)-sensitive transcripts due to the introduction of a PTC in *stipl1-1* and the T-DNA insertion in *stipl1-2*. Comparable long-period phenotypes were observed in *stipl1-1* and *stipl1-2* seedlings (Table 1; see Supplemental Figure 1D online), confirming that these mutant phenotypes are attributable to disruption of the *STIPL1* locus. However, we did not observe a rhythmic pattern of *STIPL1* transcript abundance in constant conditions (Figure 1D), suggesting that the *STIPL1* transcript itself is not subject to circadian regulation.

Sequence analysis of STIPL1 reveals that it shares significant homology with the STIP family of proteins (see Supplemental Data Set 1 online; Aravind and Koonin, 1999; Svec et al., 2004; Wang and Brendel, 2004; Ji et al., 2007) The human STIP homolog, TFIP11, has been identified as a component of spliceosomal complexes in many proteomic studies (Jurica et al., 2002; Makarov et al., 2002; Rappsilber et al., 2002; Zhou et al., 2002), thereby implicating these proteins in pre-mRNA splicing. STIPL1 is highly similar to other STIP family members, containing three conserved domains (Figure 1B) and sharing 32% overall amino acid identity and 49% similarity when compared with the human protein. STIPL1 contains two putative nuclear localization signals near the N terminus of the protein (Figure 1B; Cokol et al., 2000), and, consistent with these predicted motifs, we found STIPL1-GFP (for green fluorescent protein) to be localized to the nucleus when expressed under the control of the native *STIPL1* promoter (Figure 2A). This fusion protein also rescues the *stipl1-1* mutant phenotypes (see Supplemental Figure 1E online). STIPL1 also retains the highly conserved Gly and Tyr residues within the G-patch that are required for binding to nucleic acids (Figure 2B; Svec et al., 2004) and the conserved Gly and Phe residues within the N-terminal tuftelin-interacting protein (TIP) domain in common with other family members (Figure 2C).

stipl1 Is a Long-Period Circadian Period Mutant with Enhanced Bioluminescence

Before proceeding with additional characterization of the *stipl1-1* circadian phenotype, we backcrossed *stipl1-1* to its parental Columbia (Col) wild type five times so as to minimize the number of unlinked genetic lesions present within the *stipl1-1* germplasm. We then evaluated the *stipl1* circadian phenotype in a range of different light conditions, including constant darkness, constant red, or constant blue light. In all cases, oscillations of *CCR2*:*LUC* bioluminescence in *stipl1-1* and *stipl1-2* plants have a free-running period ~1.5 h longer than the wild type (Figure 1A, Table 1; see Supplemental Figures 1A and 1B online). As circadian rhythms may be entrained by either light or temperature cycles, we also evaluated the phenotype of *stipl1-1* mutants after growth under constant light but with regular

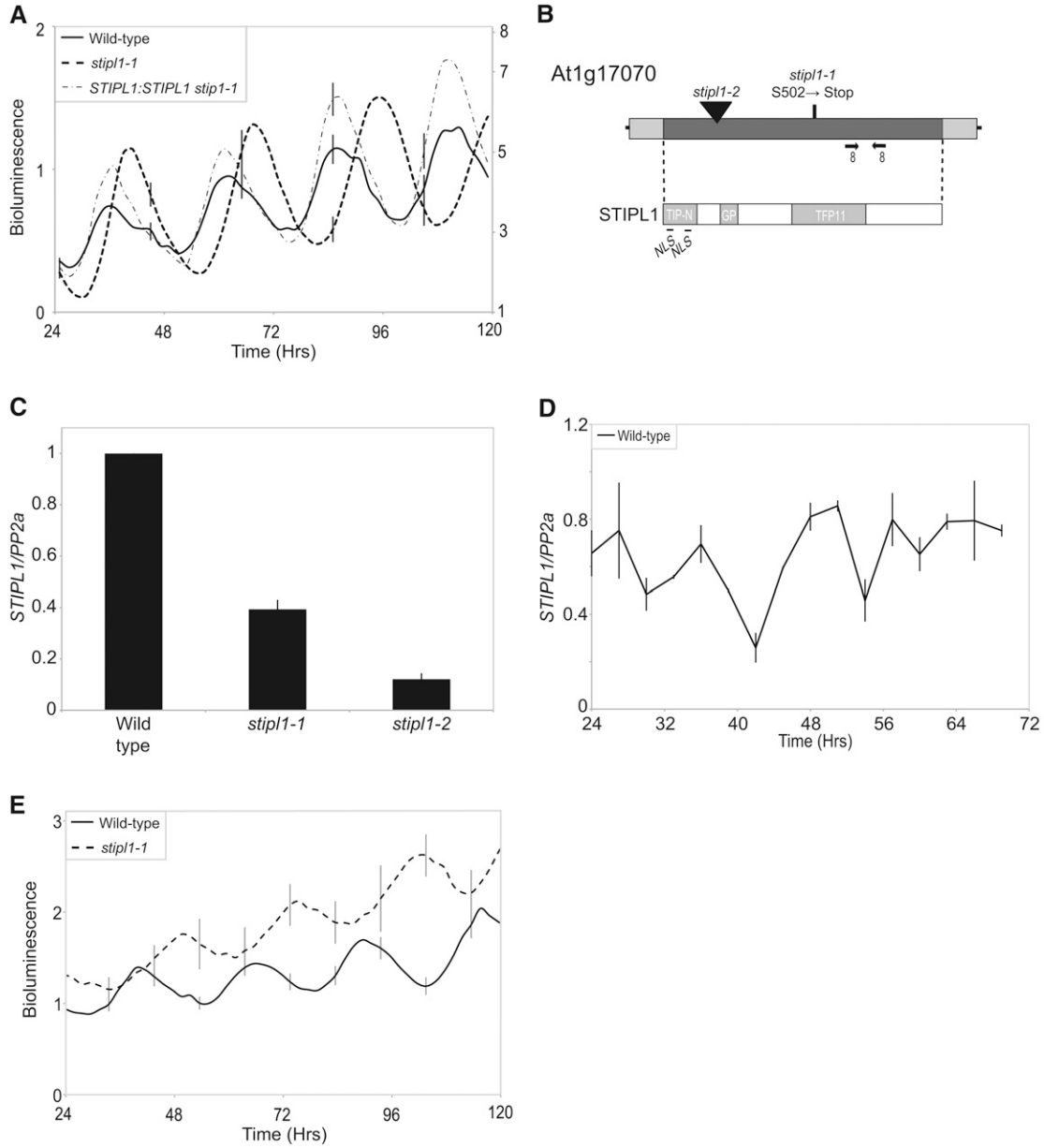

Figure 1. *stipl1* Mutant Seedlings Have a Circadian Phenotype.

(A) Bioluminescence of seedlings containing a *CCR2*:*LUC* reporter construct. Wild-type (Col; solid line), *stipl1-1* (dashed line), and transgenic plants expressing *STIPL1* under the control of its native promoter (*STIPL1*:*STIPL1 stipl1-1*, dashed-dotted line) plants were entrained to 12/12 light/dark cycles for 6 d before being moved to constant conditions with 30 μmol m^{-2} s^{-1} monochromatic red light. Error bars indicate the SE and are displayed every 20 h for clarity ($n \geq 20$). Data from *stipl1-1* plants are graphed on the secondary *y* axis on the right side of the graph.

(B) Cartoon schematic indicating position of *stipl1* mutations and the secondary structure of the STIPL1 protein, including the predicted nuclear localization signal (NLS), TIP-N, G-rich patch (GP), and TFP11 conserved domains. Positions and orientations of primers used for quantitative PCR in **(C)** are indicated by arrows.

(C) *STIPL1* transcript accumulation in wild-type (Col), *stipl1-1*, and *stipl1-2* seedlings was compared using qRT-PCR. *STIPL1* mRNA levels are presented relative to *PP2a*. Data were normalized to wild-type expression levels, and the data represent the mean of three biological replicates; SE is shown.

(D) *STIPL1* transcript accumulation over circadian time. Plants were entrained as described in **(A)** before being moved to constant white light (60 μmol m^{-2} s^{-1}). Presented data were normalized to the highest *STIPL1*/*PP2a* value and are the mean of two biological replicates; SE is shown.

(E) Bioluminescence of *stipl1-1* and wild-type *CCR2*:*LUC* seedlings following temperature entrainment. Plants were grown in 12/12 22°C/18°C cycles under white light for 6 d before being moved to constant conditions at 22°C under 30 μE red + 20 μE blue light. Error bars indicate the SE and are displayed every 20 h for clarity ($n \geq 20$).

Table 1. Circadian Period Estimates of *stipl1* and *stipl2* Mutants under Several Different Light Conditions

Light Condition	Wild Type	*stipl1-1*	*stipl1-2*	*stipl2-1*	*STIPL1:STIPL1 stipl1-1*
cR (30 μmol m^{-2} s^{-1})	24.53 ± 0.09	26.89* ± 0.08	25.97* ± 0.18	24.21 ± 0.17	24.46 ± 0.05
cB (20 μmol m^{-2} s^{-1})	24.13 ± 0.09	26.33* ± 0.12	25.57* ± 0.14	24.11 ± 0.10	24.23 ± 0.08
cR+B (30 μmol m^{-2} s^{-1} R; 20 μmol m^{-2} s^{-1} B)	24.33 ± 0.07	26.36* ± 0.07	25.51* ± 0.06	24.04 ± 0.13	24.22 ± 0.07
DD	25.15 ± 0.13	26.74* ± 0.35	ND	25.31 ± 0.12	25.05 ± 0.12

Plants were entrained as described in Figure 1A before being transferred to monochromatic red (cR; 30 μmol m^{-2} s^{-1}), blue (cB; 20 μmol m^{-2} s^{-1}), or red+blue (cR+B; 30 μmol m^{-2} s^{-1} red and 20 μmol m^{-2} s^{-1} blue) light or to constant darkness (DD). Circadian period estimates were calculated by Fourier fast transform-nonlinear least squares (Plautz et al., 1997). The mean free-running periods are indicated, ±SE. Asterisks indicate period lengths significantly different from the wild type ($P < 0.05$; $n \geq 18$). ND, not determined.

temperature cycles (22°C/17°C; Figure 1E). As for plants synchronized with light/dark cycles, *stipl1-1* mutants had a longer period than wild-type seedlings (27.18 h ± 0.29 and 25.33 h ± 0.23, respectively) when entrained with temperature cues before release to constant conditions.

To further determine the role of STIPL1 within the circadian system, we next assessed the extent to which cycling of specific clock genes was affected in *stipl1* mutants in free-running conditions using quantitative RT-PCR (qRT-PCR) to evaluate transcript oscillation over a 48-h time course in constant white light (Figure 3; see Supplemental Figure 2 online). Peak and trough expression of clock-associated genes was delayed in *stipl1-1* over the 2-d time course (Figures 3A to 3F; see Supplemental Figure 2 online), consistent with each gene cycling with a long period. However, we did not observe any defects in expression of these genes beyond this alteration of phase under these free-running conditions.

Although regulated by an endogenous oscillator, circadian clock genes are frequently also induced by environmental changes (reviewed in Harmer, 2009; Jones, 2009). This sensitivity ensures the appropriate coordination of metabolism and physiology with the environment and increases the fitness of the plant (Dodd et al., 2005). We therefore examined the expression patterns of circadian genes in *stipl1* mutants under long-day conditions (16 h light/8 h dark). In addition to the phase-shifting of clock gene transcript levels observed under constant light (Figure 3), in light/dark cycles we observed other complex effects on transcript accumulation (Figure 4). After dawn, peak levels of *LHY*, but not *CCA1*, were significantly reduced in *stipl1-1* (Figures 4A and 4B). In the morning, levels of *TOC1* and *GI* transcripts were increased in *stipl1-1* (Figures 4C and 4D), whereas the waveform of *PRR9* accumulation was delayed in *stipl1-1* mutants (Figure 4E). *PRR9* accumulation in the late night was also reduced in *stipl1* mutants, likely due to the long-period phenotype (Figure 4E). In the afternoon, peak levels of *TOC1* were slightly reduced, while the *GI* peak was delayed (Figures 4C and 4D). A similar phase delay in transcript accumulation was seen for *REVEILLE8* (*RVE8*, Figure 4F). Thus, regulation of clock gene transcript accumulation is significantly perturbed in *stipl1-1* mutants grown in light/dark cycles. Similar results were observed in *stipl1-2* mutants, although the effects of this allele were generally less severe (Figure 4).

In addition to these circadian and diurnal phenotypes, *stipl1-1* plants showed enhanced bioluminescence activity relative to the wild type in all conditions (Figure 1A; see Supplemental Figures 1A and 1B online). This phenotype was also observed when an alternate circadian reporter construct, *CCA1:LUC*, was introgressed into a *stipl1-1* mutant background (see Supplemental Figure 1C online). In an effort to further characterize this phenotype, we assessed *LUC* mRNA levels by qRT-PCR. Despite the obvious differences in bioluminescence, this analysis revealed no appreciable changes in *LUC* transcript levels compared with the wild type (see Supplemental Figure 3A online), suggesting a posttranscriptional cause for this phenotype. A similar increase in the activity of luciferase reporter genes has previously been reported for another *Arabidopsis* long-period mutant, *tej*, which encodes a poly(ADP-ribose) glycohydrolase (PARP) (Panda et al., 2002). Like *stipl1-1*, *tej* mutants do not have increased levels of endogenous *LUC* mRNAs (Panda et al., 2002), although application of the PARP inhibitor 3-aminobenzamide (3-AB) was sufficient to rescue the luminescence phenotype of the *tej* mutant. While we were able to recapitulate the phenotypic rescue of *tej* mutants following 3-AB treatment as previously described, *stipl1-1* did not show a significant response to this treatment (Panda et al., 2002; see Supplemental Figure 3B online). It therefore appears that the increased bioluminescence of *stipl1-1* mutants is neither caused by higher *LUC* gene expression nor by activation of the PARP pathway.

As the enhanced bioluminescence phenotype was not observed in *stipl1-2* plants (see Supplemental Figure 1D online), it was possible that an additional, linked mutation from the initial mutant screen might be responsible for this phenotype. To determine whether the enhanced luminescence was caused by mutation of *STIPL1*, we transformed *stipl1-1* mutants carrying the *CCR2:LUC* reporter with a wild-type copy of the At1g17070 coding region along with a 2.5-kb region of upstream genomic sequence. Seedlings homozygous for the wild-type transgene had a circadian rhythm that was comparable to the wild type in period and amplitude under all conditions tested (Figure 1A, Table 1). In addition, these plants exhibited wild-type levels of luminescence. Thus, a wild-type copy of At1g17070 rescues both the long-period and high luminescence phenotypes of

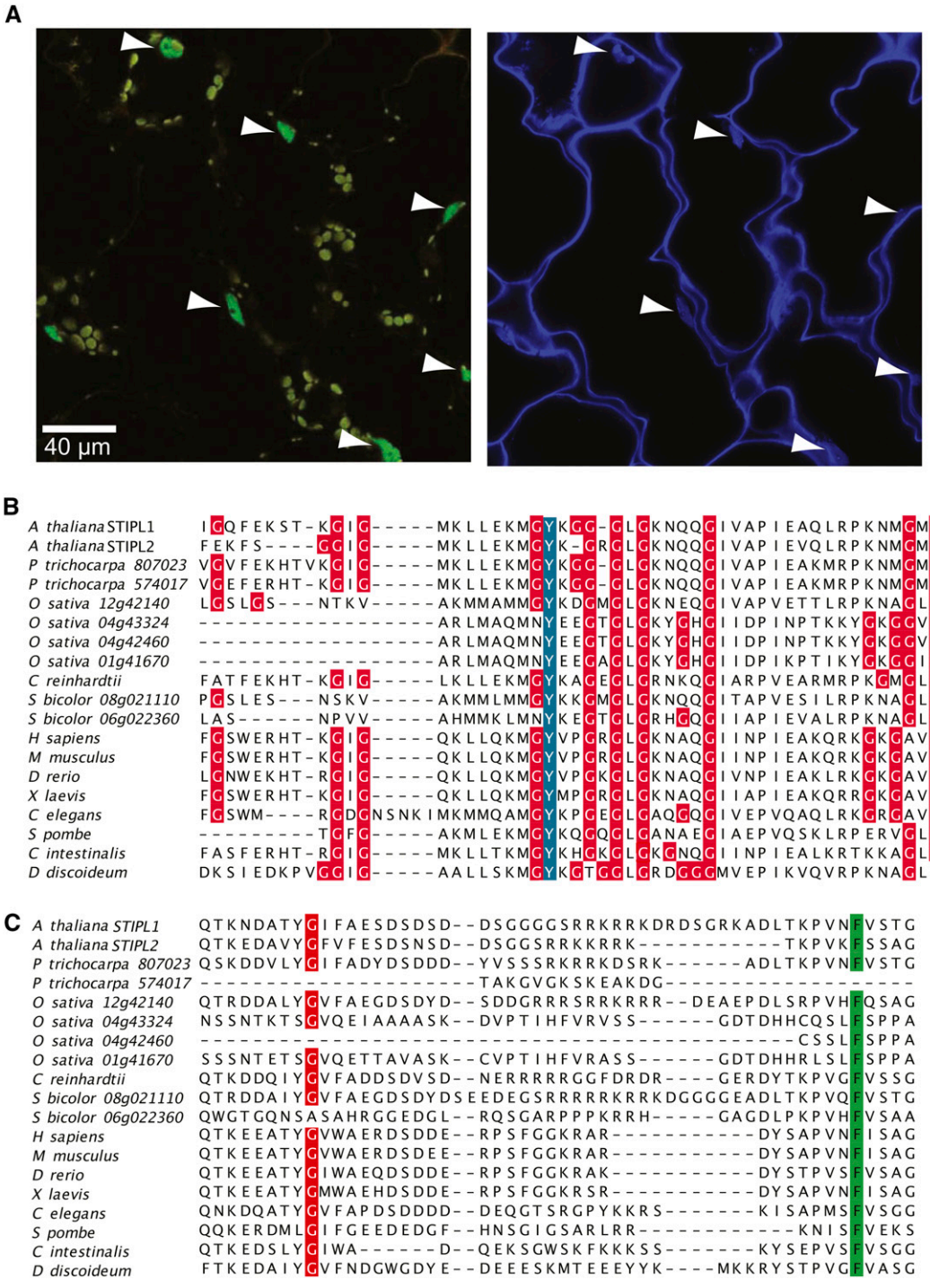

Figure 2. STIPL1 Shares Homology with STIP Family Proteins.

(A) STIPL1-GFP detection by confocal microscopy in epidermal tissue of 14-d-old seedlings expressing *STIPL1*:*STIPL1-GFP* in a *stipl1-1* background is shown on the left. Plants were grown in 12/12 light/dark cycles and examined at ZT3 (3 h after dawn). Arrowheads indicate nuclei expressing GFP. Autofluorescence from chloroplasts is evident and appears yellow in the merged image (left panel). Fluorescence following staining with DAPI is presented in the right panel (blue). DAPI staining of plant cell walls is also evident (Rost, 1995). Bar = 40 μm

(B) Residues necessary for RNA binding within the G-patch domain are conserved across diverse phyla: Gly residues are shown in red, and a conserved Tyr (Svec et al., 2004) is highlighted in blue.

(C) Conserved Gly (red) and Phe (green) residues within the TIP-N domain.

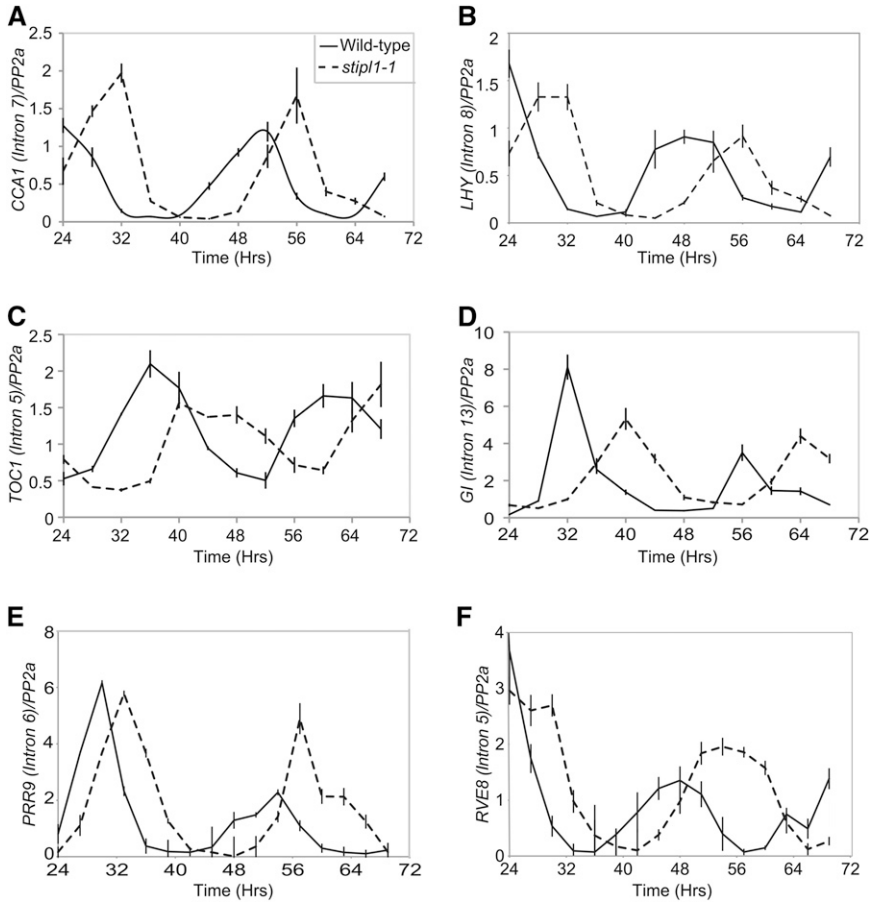

Figure 3. Expression of Circadian Clock–Regulated Genes in *stipl1* Seedlings under Constant Light.

Gene expression in the wild type (Col; solid line) and *stipl1-1* (dashed) mutants was compared using qRT-PCR. Primer pairs spanned the last intron in each gene (see *y* axis). Levels of *CCA1* **(A)**, *LHY* **(B)**, *TOC1* **(C)**, *GI* **(D)**, *PRR9* **(E)**, and *RVE8* **(F)** mRNA were assessed. Plants were entrained to 12/12 light/dark cycles for 6 d before being moved to constant conditions with 60 μmol m^{-2} s^{-1} white light. mRNA levels for each gene were normalized to *PP2a*. Data are the mean of three technical replicates; SE is shown. Results from an independent biological replicate are presented in Supplemental Figure 2 online.

stipl1-1 plants, suggesting that truncation of STIPL1 within the ethyl methanesulfonate (EMS)-generated *stipl1-1* allele has additional, genetically recessive consequences beyond the impairment of circadian function.

STIPL1 Is Required for Splicing of Circadian Clock Genes

Given the circadian phenotype and altered accumulation of some clock-related transcripts in the *stipl1* mutants, we next examined whether altered splicing patterns were observed for these genes in the mutants. Samples were collected 4 h after dawn under driven light/dark cycles (Zeitgeber time 4 [ZT4]), a time when the 3′ ends of transcripts of clock genes, such as *CCA1*, *LHY*, *TOC1*, and *GI*, show very similar expression levels in the mutant and wild type (Figure 4). Relative levels of alternatively spliced isoforms were assessed as previously described (Simpson et al., 2008; James et al., 2012). Dramatic differences were observed within the splicing variant populations of many core clock transcripts, including *CCA1*, *LHY*, *PRR9*, *GI*, and *TOC1* (Figure 5; see Supplemental Data Set 1 online). In total, we used 21 oligonucleotide pairs to evaluate splicing events across eight different clock genes (see Supplemental Data Set 2 online). Of the splicing events studied, 33% of the clock transcripts tested had significant differences in accumulation between *stipl1-1* and wild-type seedlings (>5% difference, $P < 0.05$; Table 2; see Supplemental Data Set 2 online). Similar patterns were observed in both *stipl1-1* and *stipl1-2* alleles, although differences in AS were in general slightly less severe in the latter genetic background (26% of products significantly altered; Table 2, Figure 5; see Supplemental Data Set 2 online).

Although we found that many different types of AS (intron retention, exon skipping, and alternative 5′ and 3′ splice site [SS] selection) are affected in clock genes in the *stipl1* mutants, the greatest effect is an increased abundance of transcripts with retained introns, including unspliced transcripts (Figure 5; see Supplemental Data Sets 2 and 3 online). Indeed, many intron retention transcripts observed in the *stipl1* mutants are barely visible in the wild type and other intron retention transcripts that

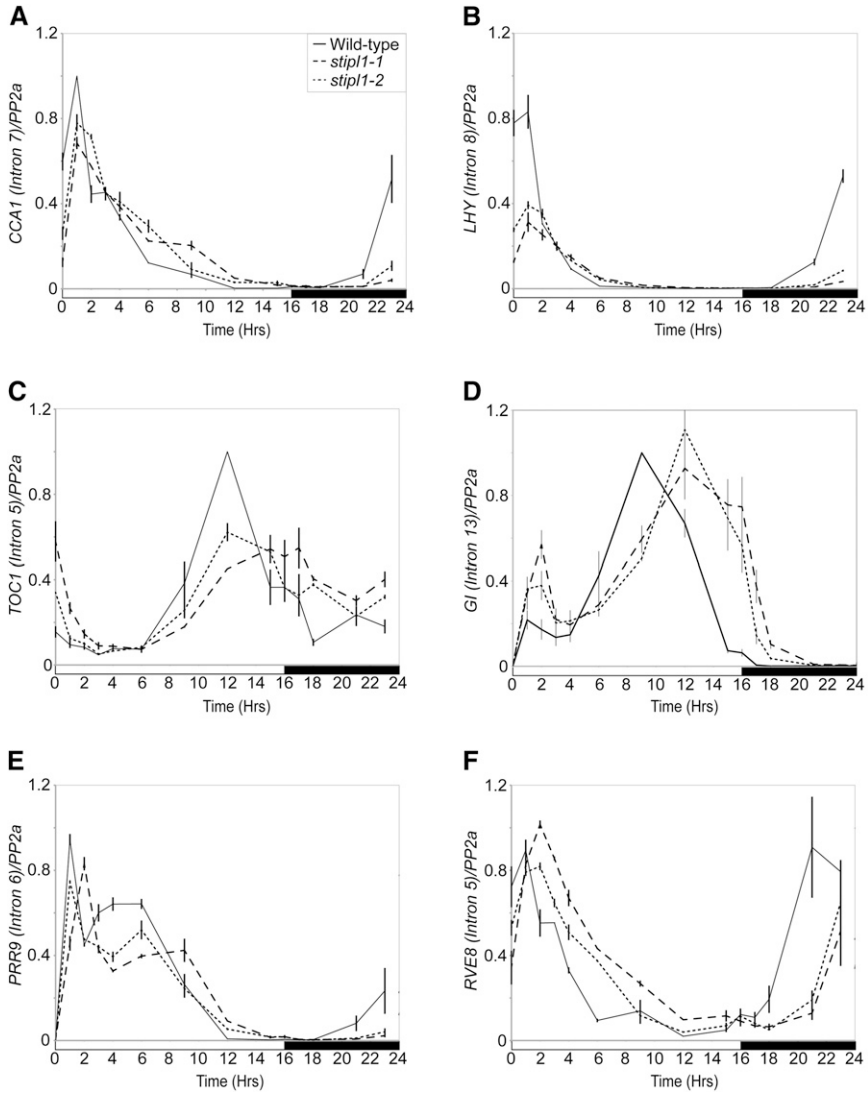

Figure 4. Abundance of Circadian Transcripts in Diurnal Conditions in *stipl1* Seedlings.

Gene expression in wild-type (Col; solid line), *stipl1-1* (dashed), and *stipl1-2* (dotted) seedlings was compared using qRT-PCR. Levels of *CCA1* **(A)**, *LHY* **(B)**, *TOC1* **(C)**, *GI* **(D)**, *PRR9* **(E)**, and *RVE8* **(F)** mRNA were assessed. Plants were entrained to 16/8 light/dark cycles with 60 μmol m^{-2} s^{-1} white light for 10 d before tissue harvesting at the indicated time point. Data for each gene were compared with an internal control (*PP2a*) before being normalized to the peak of wild-type expression. Data are the mean of at least two biological replicates; SE is shown.

are present in the wild type are increased in the mutants (see Supplemental Figure 4 and Supplemental References 1 online). To examine the general effects on splicing of the *stipl1* mutant, we also analyzed splicing/AS of a number of non-clock-related genes (see Supplemental Data Set 4 online). We surveyed 70 different genes, each with a single oligonucleotide pair. The majority showed increased levels of intron retention transcripts and unspliced transcripts with somewhat reduced levels of fully spliced (FS) mRNAs as above. A total of 35% of all the isoforms evaluated were altered by more than 5% in *stipl1-1* seedlings compared with the wild type (Table 2; see Supplemental Data Set 4 online). This suggests that the *stipl1* mutant impacts the efficiency of splicing of both constitutive and alternatively spliced introns such that a proportion of transcripts from most genes is not spliced to completion. This is also illustrated by the detection of unspliced transcripts (defined as retention of all introns within the amplified regions) in *stipl1*. In previous analyses of the non-clock genes using the same primers and range of RNAs from wild-type and various mutant plants (including serine/arginine-rich splicing factors and NMD proteins), RT-PCR products representing unspliced transcripts are usually absent or in very low abundance (Simpson et al., 2008; James et al., 2012; Kalyna et al., 2012). The increased levels of unspliced *LHY* and other transcripts in *stipl1-1* is not due to genomic DNA contamination since we were not able to amplify such products in PCR reactions using purified RNA as template (data not shown).

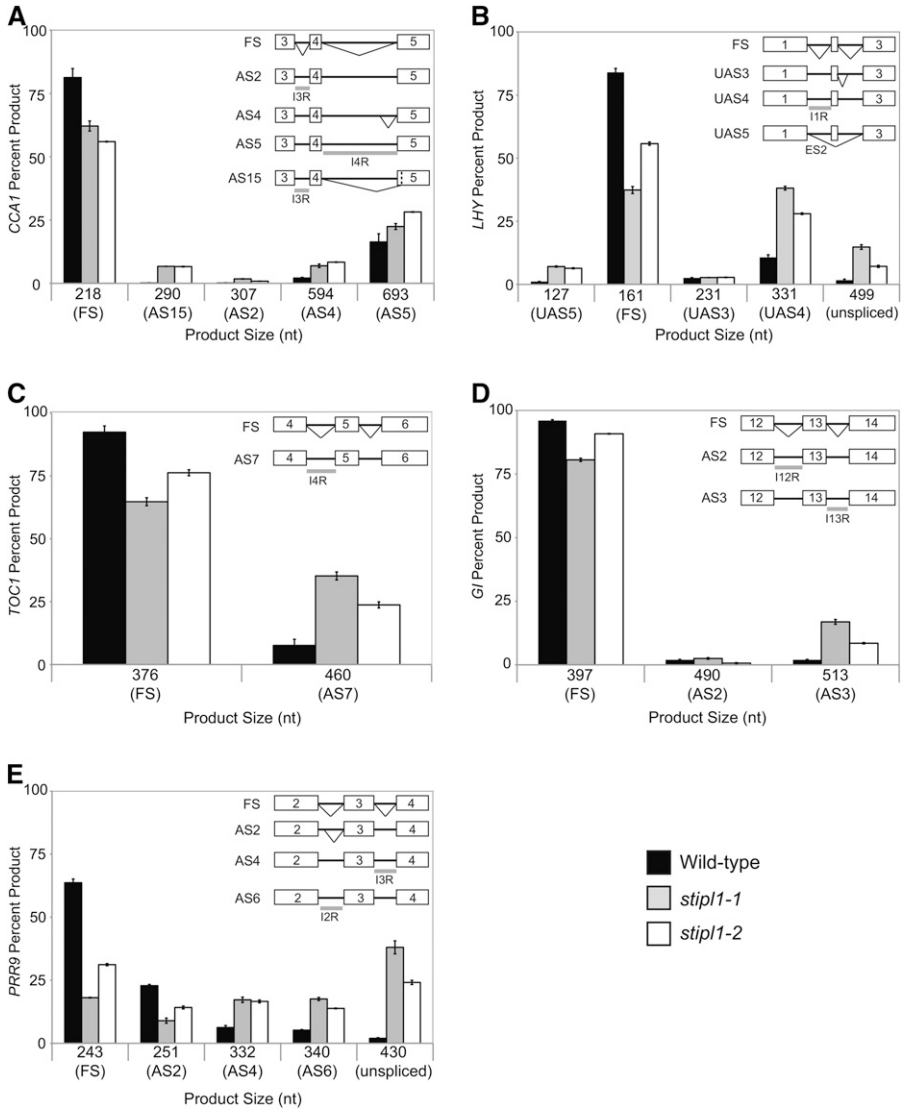

Figure 5. Examination of Circadian Gene AS Pattern Changes in *stipl1* Mutant Seedlings Using High-Resolution RT-PCR.

Plants were grown under long-day conditions (16/8 light/dark cycles) for 10 d with 60 μmol m^{-2} s^{-1} white light before being harvested at ZT4. Proportions of splice isoforms relative to the total population are presented to reflect changes in splice isoform frequency for *CCA1* **(A)**, *LHY* **(B)**, *TOC1* **(C)**, *GI* **(D)**, and *PRR9* **(E)** in wild-type, *stipl1-1*, and *stipl1-2* seedlings. Data are the mean of three biological replicates; SE is shown. The gray bars under selected introns represent intron retention events. *PRR9* splice isoforms have previously been reported as *PRR9xA* (FS), *PRR9xB* (AS2), *PRR9xC* (AS4), and *PRR9xD* (AS6) (Sanchez et al., 2010), but a revised nomenclature based upon (James et al., 2012) is used here. nt, nucleotides.

Importantly, FS transcripts remain the most abundant products, perhaps explaining why the *stipl1* splicing defect is not inherently lethal.

For the clock genes, we first examined AS changes in transcripts arising from the *CCA1* locus using primers spanning exons 3 to 5 (Figure 5A; see Supplemental Data Set 2 online). At ZT4, FS *CCA1* transcript accounts for 80% of the total population in wild-type samples, with most of the remainder (18%) identified as *CCA1* AS5, in which intron 4 is retained (James et al., 2012). By contrast, FS *CCA1* transcript only represents 58% of the total transcripts in *stipl1-1* seedlings. We identified significant increases in the proportion of *CCA1* AS5 (between 23 and 28% of the total in *stipl1* mutants) but also detected a greater proportion of *CCA1* AS4 (7% of *stipl1-1* transcripts compared with 2% in the wild type). *CCA1* AS4 is generated through the use of an alternate 5′ SS within intron 4 that increases the transcript length by 367 nucleotides (James et al., 2012). We also discovered a previously unidentified transcript not observed in the wild type, which we designate CCA1 AS15, in which intron 3 is retained and an alternate 3′ SS removes 19 nucleotides from exon 5 (Figure 5A).

Splicing defects were observed for *LHY* using primers spanning exons 1 to 3, which are all within the 5′ untranslated region (Figure 5B; see Supplemental Figures 4 and 5 and Supplemental

Table 2. Significant Changes in Proportions of Fully and Alternatively Spliced Transcripts in *stipl* Mutants

	No. of Transcripts (FS and AS) with Significant Changes (%)	
Genotype	3–5% change; $p<0.05$	>5% change; $p<0.05$
Clock genes[a]		
stipl1-1	41%	33%
stipl1-2	30%	26%
stipl2-1	2%	2%
Other genes[b]		
stipl1-1	42%	35%
stipl1-2	39%	32%
stipl2-1	2%	1%

Plants were grown and RNA isolated as described in Figure 5.

[a]A subset of eight genes ascribed a role within the circadian system were assayed using 21 oligo pairs (generating 91 distinct transcripts) for *stipl1-1* and *stipl1-2* or 20 oligo pairs (generating 87 distinct transcripts) for *stipl2-1*.

[b]Seventy genes with a total of 268 transcripts (assayed using 70 oligo pairs) were scored for all three mutants. Data for individual oligo pairs are provided in Supplemental Data Sets 2 to 6 online.

Data Sets 2 and 3 online). The FS transcript (161 nucleotides) accounts for 82% of the total product in the wild type, with a smaller fraction represented by *LHY* UAS4 in which intron 1 in the 5′ untranslated region is retained (10% of total; James et al., 2012). In *stipl1-1* plants, we observed a reduction in the proportion of the FS transcript (37% of total) and corresponding increases in the *LHY* UAS4 isoform (37% of total), of UAS5 (exon 2 skip), and unspliced product (499 nucleotides, 15% of total).

Previous work describing *PRR9* has identified two AS events (an alternative 5′ SS in intron 2 adding 8 nucleotides to the transcript and retention of intron 3), generating four AS transcript variants across exons 2, 3, and 4 (Sanchez et al., 2010). We identified each of these isoforms in wild-type and *stipl1* mutant plants (Figure 5E; see Supplemental Data Set 2 online) but also detected significant quantities of unspliced product in *stipl1-1* mutants (428 nucleotides, 38% of total in *stipl1-1*; see Supplemental Data Set 3 online). As for other examined genes, the proportion of transcripts retaining intron 3 increased in *stipl1* mutants (*PRR9* AS4 and *PRR9* AS6; Figure 5E; see Supplemental Figure 5C online) with a commensurate decrease in the proportion of transcripts in which this intron was removed (FS *PRR9* and *PRR9* AS2). In contrast with what we observed for these other clock genes, there was no significant change in AS ratios for *PRR7* transcripts in the *stipl1* mutants (see Supplemental Figure 4D online).

Although we collected samples during the morning (at ZT4), we were also able to detect alterations in AS transcript accumulation for evening phased genes despite their low levels of expression. When we examined AS across exons 12 to 14 of *GI* in *stipl1* seedlings (Figure 5D; see Supplemental Data Set 2 online), we observed increased levels of *GI* AS3 (513 nucleotides, 8 to 17% of total), in which intron 13 is retained. We also observed perturbations in *TOC1* AS isoforms, with *TOC1* AS7 (retention of intron 4) representing 24 to 35% of the total detected transcript in the mutant compared with 8% in the wild type (Figure 5C; see Supplemental Data Set 2 online). These data indicate that the splicing defect observed in the *stipl1* mutants affects the relative proportions of FS and alternatively spliced isoforms of many, although not all, core clock genes.

We also examined relative levels of each AS isoform following normalization to *UBIQUITIN-CONJUGATING ENZYME21* (*UBC21*). In particular, FS *LHY* and *PRR9* are reduced approximately twofold (see Supplemental Figures 5B and 5C online), but FS *CCA1* is not significantly changed in *stipl1-1* seedlings compared with the wild type (see Supplemental Figure 5A online). In addition, expression of FS *GI* is increased in *stipl1* mutant plants, although relative levels of this evening-phased gene remain low compared with morning-phased genes, such as *CCA1* and *LHY* (see Supplemental Figure 5D online). The decrease in levels of FS transcripts for *LHY* may be due to increased abundance of AS, but this is unlikely to explain the increase in *GI* transcripts as AS events are in low abundance.

Consistent with the selective effect of loss of STIPL1 function on splicing of clock genes, many AS events are not altered in *stipl1* mutants (see Supplemental Figures 4D and 6 and Supplemental Data Set 2 online). Therefore, disruption of the *STIPL1* locus causes a range of defects within both AS isoform population composition and FS transcript abundance for multiple clock genes, all of which may contribute to the observed long-period phenotype.

STIPL2, a STIPL1 Paralog, Has neither a Circadian Defect nor Altered Accumulation of Clock-Related Transcripts

STIP proteins have previously been described as single-copy genes found throughout the metazoa, although higher plants were not included in this survey (Ji et al., 2007). Our phylogenetic analysis (Figure 6A; see Supplemental Data Set 1 online) reveals that *Arabidopsis* contains two *STIP* paralogs, *STIPL1* and a related gene that we call *STIPL2* (At2g42330); STIPL1 and STIPL2 are 61% identical and 72% similar at the amino acid level. Similarly, two paralogs were identified in moss (*Physcomitrella patens*), *Populus trichocarpa*, and *Sorghum bicolor*, whereas four paralogs were identified in rice (*Oryza sativa*). Our analysis suggests that duplication of this gene occurred independently in each of these lineages (Figure 6A). However, duplication of these genes has apparently not occurred in all plant species as only a single *STIP* homolog was identified in maize (*Zea mays*; Figure 6A). Both *STIPL1* and *STIPL2* are expressed throughout development (see Supplemental Figure 7 online), and as for *STIPL1*, we found that *STIPL2* is not rhythmically expressed under constant conditions (Figure 6B). To ascertain whether *stipl2* mutants also have a circadian defect, we obtained a GABI-Kat T-DNA line (Li et al., 2007) with an insertion within this gene that we named *stipl2-1* (Figure 6C). Once we confirmed that *STIPL2* expression was impaired (Figure 6D), we crossed the *CCR2*:*LUC* reporter into this mutant background and found the free-running period to be the same as the wild type (Table 1, Figure 6E). This suggests that STIPL1 but not STIPL2 is essential for maintenance of the circadian system.

As partial redundancy of function is frequently observed within gene families in *Arabidopsis*, we attempted to isolate a *stipl1*

stipl2 double mutant to determine whether these plants had an exacerbated circadian phenotype. We crossed *stipl1-2* and *stipl2-1* to each other and examined segregation of the mutant alleles in the resulting F2 progeny. Despite examining 114 seedlings, we were unable to identify any *stipl1 stipl2* double mutant plants. Furthermore, no plants heterozygous for *stipl1-2* and homozygous for *stipl2-1* were obtained, although we did isolate a small number of plants homozygous for *stipl1-2* and heterozygous for *stipl2-1* (Table 3). This skewing of the expected segregation ratios is highly significant ($P < 0.001$) and indicates that a copy of either STIPL1 or STIPL2 is required for plant viability.

Since STIPL2 is a paralog of STIPL1 that does not have a mutant circadian phenotype (Table 1, Figure 6E), we examined whether *stipl2-1* seedlings displayed altered accumulation of circadian transcripts (Figure 7). Using primers specific for the FS transcripts described in Figure 5, we found that the wild-type FS transcript abundance closely matched the results obtained using primers in the 3′ end of transcripts (Figure 4), but we did observe an increased peak level of FS *TOC1* transcript in this line (Figure 7C). However, the phase of *TOC1* expression (and that of the other clock genes assessed) remains unchanged, consistent with the normal period phenotype in these plants (Table 1, Figure 6E). To examine whether STIPL2 affects constitutive or alternative splicing, we examined the transcript profiles of 78 clock and non-clock-associated genes in *stipl2-1* (Table 2; see Supplemental Data Sets 5 and 6 online). The striking increases in abundance of intron retention and unspliced transcripts seen with the *stipl1* mutants are absent (see Supplemental Figure 4 online). Only 2% of isoforms analyzed display a significant difference in accumulation between *stipl2-1* and the wild type (>5% difference, $P < 0.05$; Table 2). Therefore, STIPL2 has no effect on splicing efficiency of the majority of genes/transcripts analyzed. These data reinforce our finding that STIPL1 has a general function in the splicing process and plays a predominant role in AS events in clock transcripts (see Supplemental Data Set 2 online) and suggests that STIPL2 may only affect a small subset of introns/genes (see Supplemental Data Sets 5 and 6 online). Therefore, despite the homology between STIPL1 and STIPL2 and their possible partial functional redundancy (suggested by our inability to isolate *stipl1 stipl2* mutants), these related genes have diverged functions and very different impacts on the circadian system.

DISCUSSION

Mutation of *STIPL1* Enhances Luciferase Bioluminescence

Although the primary intent of our mutant screen was to identify novel components of the *Arabidopsis* circadian system, our methodology also allowed us to identify mutants with altered bioluminescence activity (Figure 1A). Our rescue of the wild-type luminescence phenotype in *stipl1-1* with a genomic insert encompassing the *STIPL1* gene confirms that the increased luminescence is due to disruption of this locus. The normal *LUC* transcript levels in this mutant (see Supplemental Figure 3A online) indicate that the enhanced brightness is not a consequence of enhanced transcription rates within the *stipl1-1* mutant. Similar increases in bioluminescence have previously been reported for the *tej* mutant, which encodes a defective poly-(ADP-ribose) glycohydrolase (Panda et al., 2002). However, it appears that *stipl1-1* phenocopies *tej* via an alternate mechanism as treatment with 3-AB fails to reduce the bioluminescence of *stipl1* mutants as reported for *tej* (Panda et al., 2002; see Supplemental Figure 3B online). Investigation of the mechanisms underlying the increased luminescence activity of the *stipl1-1* allele will be a focus of future research.

STIPL1 and *STIPL2* Are Members of the STIP Family

Sequence homology places STIPL1 and STIPL2 within the STIP family of RNA binding proteins, which are found in all examined eukaryotes (Figure 6A; Ji et al., 2007). Both STIPL1 and STIPL2 contain the conserved TIP-N, G-patch, and TFP11 domains commonly associated with this protein family (Figures 1B, 2B, and 2C). G-patch domains are short, Gly-rich sequences that possess RNA binding activity and are found in a number of proteins involved in RNA processing (Aravind and Koonin, 1999; Svec et al., 2004). The six most highly conserved Gly residues that give the G-patch domain its name are present in both STIPL1 and STIPL2 and also conserved is a Tyr that is required for binding to nucleic acids (Svec et al., 2004; Figure 2B). The TFP11 domain is named for the human protein TFIP11 (Paine et al., 2000) and is unique to STIP family members (Ji et al., 2007). Within the TFP11 domain is a short speckle-targeting sequence that is responsible for the subnuclear speckling of TFIP11 (Tannukit et al., 2009). This region is not retained in STIPL1 nor in STIP family members outside the examined chordates (see Supplemental Data Set 1 online). In the STIPL1-GFP *Arabidopsis* lines, STIPL1 localized to the nucleus with little evidence of localization to subnuclear speckles (Figure 2A).

STIP proteins have previously been described as essential, single-copy genes found throughout the animalia (Ji et al., 2007). Our phylogenetic analysis suggests that this family has undergone multiple independent duplication events in plants (Figure 6A). Despite this, our inability to isolate *stipl1 stipl2* double mutants (Table 3) suggests that the requirement of *STIP* gene function for viability is retained across both animals and plants. In addition, the absence of *stipl1*+/− *stipl2*−/− but not *stipl1*−/− *stipl2*+/− seedlings suggests that STIPL2 may play a more critical role in plant growth and development than STIPL1. The circadian phenotype seen in *stipl1* but not *stipl2* mutants and the upregulation of *STIPL2* expression in maturing seeds (see Supplemental Figure 7 online) provide further evidence that these genes have evolved specialized functions. The gene duplication events observed in plants will enable further functional characterization of these essential proteins in vivo, and it will be of interest to determine whether STIPL1 paralogs in other plant species have similarly evolved specialized functions in each of these lineages.

Defective Splicing Events May Contribute to Circadian Period Lengthening in *stipl1* Seedlings

The sequence conservation of *Arabidopsis* STIPL1 and STIPL2 with other eukaryotic proteins, such as human TFIP11 (a

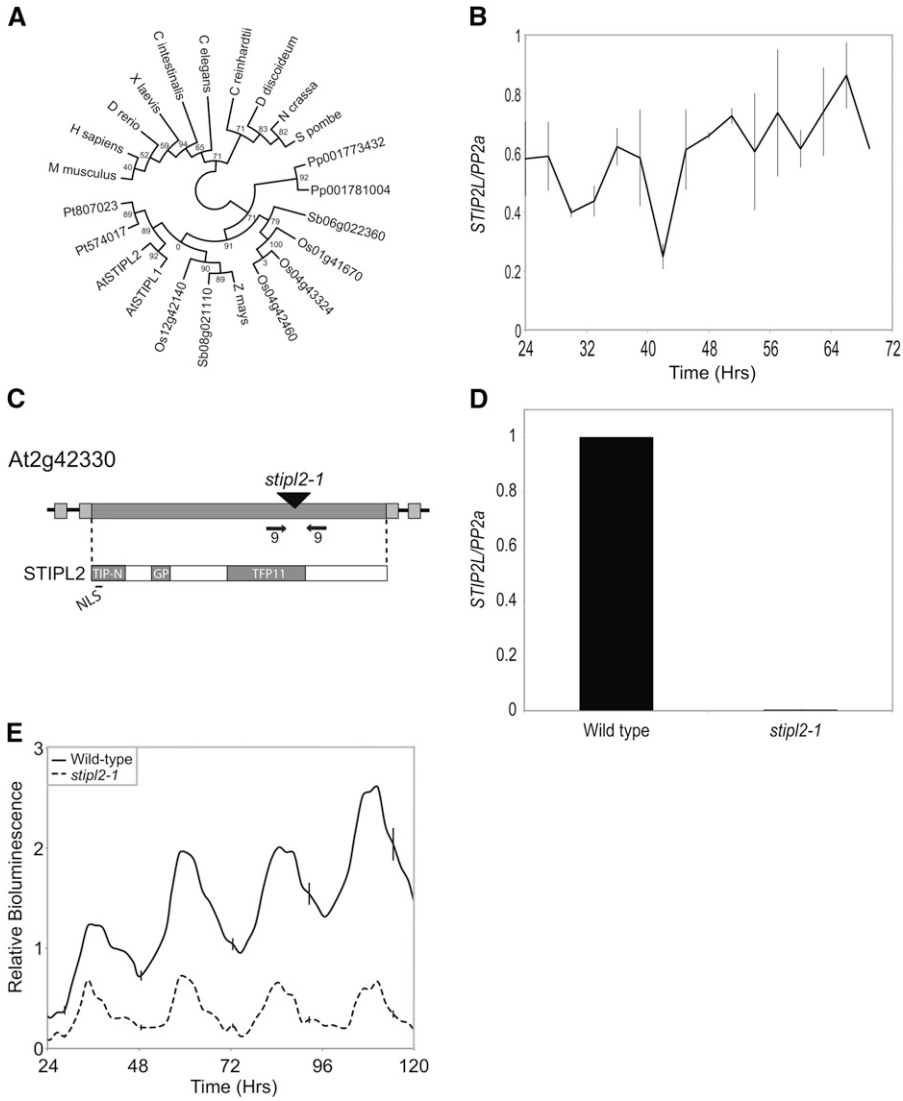

Figure 6. STIPL2 Is a Paralog of STIPL1 in *Arabidopsis*.

(A) Cladogram displaying *STIPL1* homologs in a broad range of phyla. *Arabidopsis STIPL1* has a close paralog, *STIPL2* (At2g42330). Where multiple homologs were identified within a single species, the annotated gene model code is provided. Sb, *Sorghum bicolor*; Os, *Oryza sativa*; Pt, *Populus trichocarpa*; Pp, *Physcomitrella patens*. Percentage bootstrap values are presented for each node.

(B) *STIPL2* transcript accumulation over circadian time. Plants were entrained as described in Figure 1A before being moved to constant white light (60 μmol m^{-2} s^{-1}). Presented data were normalized to the highest *STIPL2*/*PP2a* value and are the mean of two biological replicates; SE is shown.

(C) Cartoon schematic indicating position of T-DNA insertion and the secondary structure of the STIPL2 protein, including the predicted nuclear localization signal (NLS), TIP-N, G-rich patch (GP), and TFP11 conserved domains. Positions and orientations of primers used for quantitative PCR in **(B)** and **(D)** are indicated by arrows.

(D) *STIPL2* transcript accumulation in wild-type (Col) and *stipl2-1* seedlings was compared using qRT-PCR. *STIPL2* mRNA levels were compared with *PP2a* before being normalized to wild-type expression levels. Data are the mean of three independent biological replicates; SE is shown.

(E) Bioluminescence of seedlings containing a *CCR2:LUC* reporter construct. Wild-type (Col; solid line) and *stipl2-1* (dashed line) plants were entrained to 12/12 light/dark cycles for 6 d before being moved to constant conditions with 30 μmol m^{-2} s^{-1} monochromatic red light. The reduced activity of the luciferase transgene seen in *stipl2-1* is frequently observed in T-DNA mutants from the GABI collection (Martin-Tryon et al., 2007; Daxinger et al., 2008; Jones et al., 2010). Error bars indicate SE and are displayed every 20 h for clarity ($n \geq 27$).

spliceosomal protein involved in spliceosome disassembly; Tannukit et al., 2009), indicates that we have identified a plant homolog of TFIP11. STIPL1 homologs from humans and *Drosophila melanogaster* are able to rescue developmental defects in *Neurospora crassa*, suggesting a conservation of function (Ji et al., 2007). Although mutation of the STIPL1 paralog STIPL2 does not cause a widespread decrease in splicing efficiency or a circadian phenotype (Figures 6E and 7, Table 1; see Supplemental Data Sets 5 and 6 online), the synthetic lethality of the *stipl1 stipl2* double mutants (Table 3) argues that both proteins retain

Table 3. Genotyping of *stipl1* × *stipl2* Mutant Crosses

Genotype	*STIPL1/STIPL1*	*STIPL1/stipl1-2*	*stipl1-2/stipl1-2*
STIPL2/STIPL2	14	16	33
STIPL2/stipl2-1	18	20	7
stipl2-1/stipl2-1	6	0	0

A total 114 F2 progeny from a *stipl1-2* × *stipl2-1* cross were genotyped using primers described in Supplemental Data Set 8 online. Total numbers for each observed allele combination are presented.

spliceosomal functions in plants but have partially diverged functions. Although *STIPL2* transcript is readily detectable in seedlings (Figures 6B and 6D), publically available microarray data suggest that *STIPL2* transcript levels are higher in seed (see Supplemental Figure 7 online). A key role for STIPL2 for correct splicing of essential gene(s) during embryo development might explain our inability to recover *stipl1 stipl2*.

While circadian clocks are thought to have arisen independently in higher taxa, they typically share overarching mechanisms to achieve similar regulatory effects (Rosbash, 2009). Throughout the day, circadian transcripts generated by differential gene expression are further regulated by AS, NMD, and altered stability (Staiger and Green, 2011). In the green alga *Chlamydomonas reinhardtii*, an RNA binding protein, CHLAMY1, is necessary for the maintenance of circadian rhythms (Iliev et al., 2006). Similarly, a *Drosophila* RNA binding protein, LARK, has also been assigned a role in this circadian system (Huang et al., 2007). More recently, PRMT5 and SKIP have been shown to modulate the *Arabidopsis* circadian clock in part by increasing the level of unproductive AS isoforms of *PRR9* relative to FS mRNAs (Hong et al., 2010; Sanchez et al., 2010; Wang et al., 2012), although *skip* alters the 5′ and 3′ SS selection of many genes (Wang et al., 2012). Both *prmt5* and *skip* greatly increase transcripts in which intron 3 is retained and promote the use of an alternative 5′ SS in intron 2 that places the transcript out of frame (Sanchez et al., 2010; Wang et al., 2012). As *prmt5*, *skip*, and *stipl1* mutants have a long-period phenotype and display increased accumulation of *PRR9* isoforms in which intron 3 is retained (Figure 5; Sanchez et al., 2010; Wang et al., 2012), it is tempting to speculate that the altered waveform of FS *PRR9* mRNAs (Figure 7E) may play a role in the long-period phenotype of *stipl1*. However, the alteration in the composition of the AS population at ZT4 (Figure 5) and differences in FS accumulation over diurnal time for multiple clock genes in *stipl1* alleles (Figure 7) instead suggest that altered splicing of many clock-associated transcripts all contribute to its circadian dysfunction. Indeed, we cannot distinguish between those mutant phenotypes that are contributive or consequential of the observed circadian defects.

Several recent studies have revealed that many clock genes generate unproductive alternatively spliced isoforms (introducing PTCs into the mature transcript), that many such transcripts are NMD sensitive, and that the ratio of these isoforms may change over diurnal time and due to environmental stress (Filichkin et al., 2010; Sanchez et al., 2010; Filichkin and Mockler, 2012; James et al., 2012). The alternatively spliced isoforms showing the greatest increase in abundance in the *stipl1* mutants are intron retention/unspliced transcripts that contain PTCs (Figure 5). In plants, many transcripts with retained introns appear insensitive to NMD (Marquez et al., 2012). Although we do not yet understand the fate of such transcripts, they and other AS transcripts potentially encode truncated proteins that may or may not be functional. For example, *CCA1* AS15 would produce a 51–amino acid peptide, while *PRR9* AS4, *PRR9* AS6, *GI* AS3, and *TOC1* AS7 (each of which form a greater proportion of the total transcript pool in *stipl1* mutants than in the wild type; Figure 5) could similarly generate N-terminally truncated proteins. It was recently suggested that the *CCA1* AS5 (intron 4 retained) isoform encodes a C-terminal truncated *CCA1* protein that lacks the N-terminal MYB domain and which represses the function of the full-length protein, although it is not yet clear whether this truncated protein is normally produced (Seo et al., 2012). Although beyond the scope of this study, it will be of great interest to determine whether truncated proteins are generated from unproductive AS isoforms and have a function in circadian control.

Although we observed a delayed accumulation of multiple transcripts under diurnal conditions that is consistent with the long-period phenotype observed under constant conditions (Figures 1A, 4, and 7; see Supplemental Figure 1 online), our data cannot simply be explained by the increase in period length. A recent study has cataloged the diversity of circadian transcripts generated by AS and demonstrated that other intron retention events, such as *LHY* UAS4 and *TOC1* AS7, transiently accumulate following the transfer of plants to 4°C (James et al., 2012). Our study similarly reveals upregulation of the *LHY* UAS4 and *TOC1* AS7 isoforms in *stipl1* mutant plants (Figures 5B and 5F), while we also observe a reduction in the proportion of the FS *LHY* and *TOC1* transcripts (Figures 4B and 4C). James et al. (2012) suggest that both of these isoforms are susceptible to NMD, perhaps due to the arrangement of upstream open reading frames (in *LHY*). The observed reduction in levels of FS *LHY* and *TOC1* transcripts (Figures 7B and 7C) in *stipl1* mutants may be indicative of this process in these seedlings.

stipl1 seedlings have a longer circadian period following entrainment to either light or temperature cues (Figures 1A and 1E), suggesting that STIPL1 acts upon the molecular oscillator itself rather than by altering either light or temperature input components. However, we do not suggest that STIPL1 is a canonical core clock component as its expression is not itself clock regulated (Figure 1D) nor is its expression significantly altered by application of environmental stresses (Killian et al., 2007; see Supplemental Data Set 7 online). Instead, STIPL1 is involved in efficient splicing of introns in the majority of genes examined. In the mutant, while most genes/introns are affected, the largest proportion of transcripts is correctly spliced to mature, protein-coding mRNAs. Splicing in humans and yeast is thought to be largely cotranscriptional, with the rate of transcription affecting alternative SS choice and feedback from the splicing process affecting transcription (McCracken et al., 1997; Alexander et al., 2010; Luco et al.,

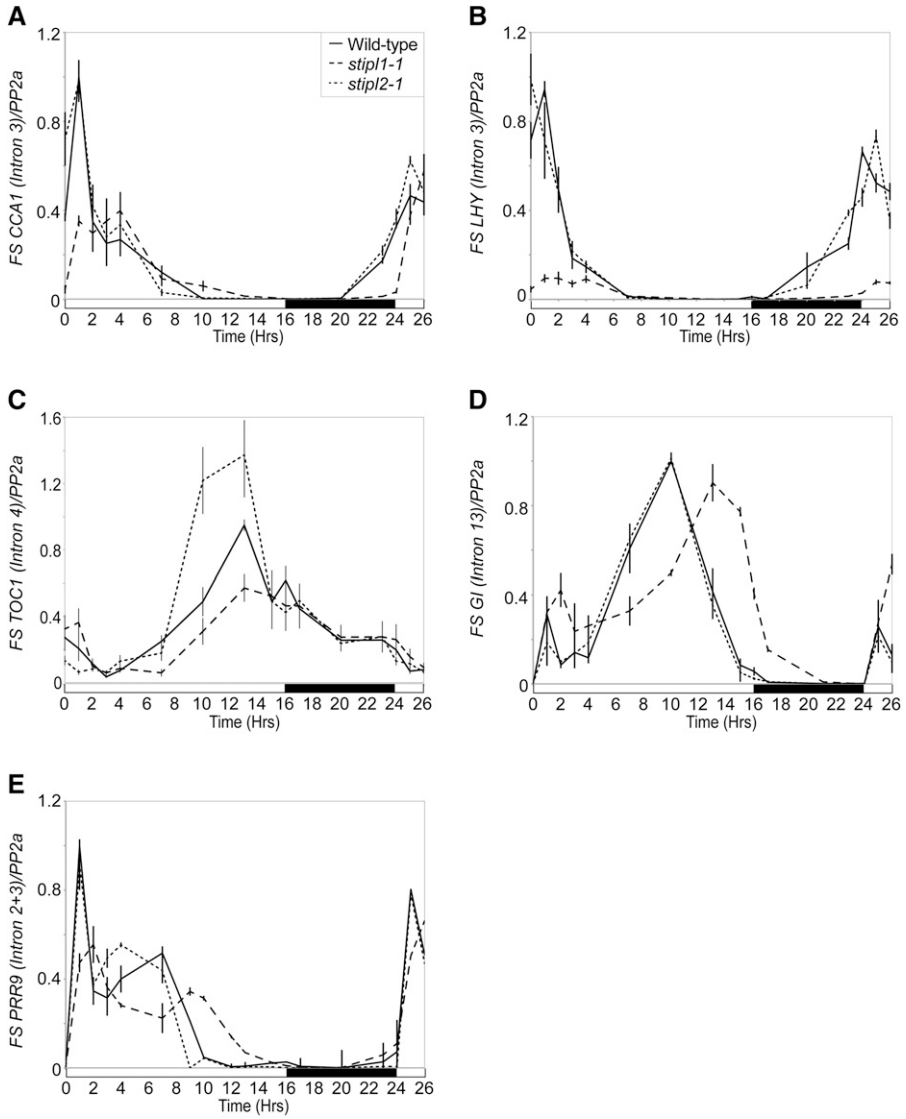

Figure 7. Expression of Circadian Clock–Regulated Genes in *stipl1* and *stipl2* Mutant Seedlings under Long-Day Conditions.

Gene expression in wild-type (Col; solid line), *stipl1-1* (dashed), and *stipl2-1* (dotted) seedlings was compared using qRT-PCR using primers specific for FS transcripts. Levels of *CCA1* **(A)**, *LHY* **(B)**, *TOC1* **(C)**, *GI* **(D)**, and *PRR9* **(E)** mRNA were assessed. Plants were grown under long-day conditions (16/8 light/dark cycles) for 10 d under 60 μmol m^{-2} s^{-1} white light. mRNA levels for each gene were normalized to that of *PP2a*. Data for each gene were compared with an internal control (*PP2a*) before being normalized to the peak of wild-type expression. Data are the mean of at least two biological replicates; SE is shown.

2010; Luco and Misteli, 2011). We do not yet know whether such interactions occur in plants, but it seems likely to be the case, and we also do not understand how the inefficient splicing seen in the *stipl1* mutants manifests itself at the molecular level. However, the increased abundance of AS variants may be related to reduced efficiency of completion of the splicing process. Whatever the mechanism, mutation of STIPL1 ultimately affects AS of clock gene transcripts and resulting levels of functional mRNAs. In addition, mutation of *STIPL1* does not affect all splicing events to the same extent (see Supplemental Data Sets 2 to 4 online), which may reflect features of different introns, such as the strength of splicing signals or secondary structure. Finally, the splicing phenotypes of the *stipl1* and *stipl2* mutants are significantly different, with *STIPL2* only affecting expression of one of the clock genes analyzed (Figure 7), consistent with the lack of a period phenotype. Our data clearly emphasize the importance of splicing and AS in the control of the circadian system. Future work will examine a possible role for STIPL1 in spliceosome disassembly and further investigate how altered splicing of circadian transcripts perturbs the function of the circadian clock.

METHODS

Plant Materials and Growth Conditions

The *stipl1-1* EMS allele was isolated from a previously described mutant population (Martin-Tryon et al., 2007). In brief, *Arabidopsis thaliana* (Col ecotype) plants transformed with the *CCR2:LUC* reporter construct (Strayer et al., 2000) were mutagenized with EMS before M2 seeds were screened for defective circadian rhythms under constant darkness (Harmer and Kreps, 2002). *stipl1-1* seeds were backcrossed to Col for three generations before being outcrossed to Landsberg *erecta* to generate a mapping population. A total of 1576 plants from the F2 mapping population were screened using bulk segregant analysis and simple sequence length polymorphic mapping methods (Lukowitz et al., 2000; Martin-Tryon et al., 2007) that linked the causative locus to a 46.5-kb region on chromosome 1. Sequencing of candidates within this region (see Supplemental Table 1 online) revealed a G→A substitution generating a PTC within At1g17070.

stipl1-2 (SAIL-073187) and *stipl2-1* (GABI-425C03) seeds were obtained from the SAIL and Gabi-Kat T-DNA insertion collections, respectively (Sessions et al., 2002; Li et al., 2007). Homozygous T-DNA insertion lines were verified using primer sets 1 to 4 as described in Supplemental Data Set 8 online. Transgenic plants were generated by introducing the *STIPL1* coding sequence and a 2.5-kb region upstream of the transcriptional start site into pENTR-D/TOPO (Invitrogen) via the TOPO cloning method and primer set 5 (see Supplemental Data Set 8 online). A binary vector containing the *STIPL1* genomic fragment was created by LR recombination with pEG301 (Earley et al., 2006). A similar vector containing this genomic fragment and a C-terminal GFP fusion was created by LR recombination with pGWB4 (Nakagawa et al., 2007). pEG301 STIPL1 and pGWB4 STIPL1 were moved into *Agrobacterium tumefaciens* strain GV3101 and transformed into *stipl1-1* plants using standard protocols (Clough and Bent, 1998). Transformants were selected on Murashige and Skoog media supplemented with 75 μg/mL kanamycin (Fisher Scientific).

Luciferase Imaging Assays

Plants were entrained for 6 d in 12/12 light/dark cycles under white light on Murashige and Skoog media supplemented with 3% Suc before being sprayed with 3 mM D-luciferin in 0.01% Triton X-100. Plants were then transferred to free-running conditions under either red, blue, or red+blue light-emitting diodes or held in constant darkness as previously described (Jones et al., 2010). Imaging was completed over 5 d, and data was processed using Metamorph software (Molecular Devices). Patterns of luciferase activity were fitted to cosine waves using Fourier fast transform-nonlinear least squares (Plautz et al., 1997) to estimate circadian period length.

The 3-AB treatment protocol was modified from Panda et al. (2002). Plants were entrained to 12/12 light/dark cycles before being sprayed with a combination of 3 mM D-luciferin and 8 mM 3-AB in 0.01% Triton X-100. Plants were then returned to diurnal cycles for 24 h before being transferred to constant red light for luciferase imaging for 5 d.

qRT-PCR

RNA was isolated and qRT-PCR performed as previously described (Jones et al., 2010). Briefly, total RNA and cDNA synthesis were completed using TRIzol reagent and SuperScript II reverse transcriptase, respectively, following the manufacturer's protocol (Invitrogen). Real-time qRT-PCR was performed in 40 mM Tris-HCl, pH 8.4, 100 mM KCl, 6 mM MgCl2, 8% glycerol, 20 nM fluorescein, 0.4× SYBR Green I (Molecular Probes), 1× BSA (New England Biolabs), 1.6 mM deoxynucleotide triphosphates, 2.5 mM each primer, and 5% diluted cDNA using Taq polymerase. Samples were run in triplicate, with starting quantity estimated from critical thresholds using the standard curve of amplification. Data for each sample were normalized to *PP2a* expression as an internal control. Primer sets used are described in Supplemental Data Set 8 online.

High-Resolution RT-PCR

High-resolution RT-PCR was performed as previously described (Simpson et al., 2008; James et al., 2012). Briefly, 4 μg of total RNA was used in first-strand cDNA synthesis by reverse transcription with oligo$(dT)_{18}$ using Ready-To-Go You-Prime First-Strand Beads (GE Healthcare) in a final volume of 20 μL. Gene-specific primer pairs (with one 6-carboxyfluorescein–labeled primer; see Supplemental Data Set 8 online) were designed to amplify between 400 and 800 bp to capture different splicing events. RT-PCR was performed as described (Simpson et al., 2008). The resultant RT-PCR products representing AS transcripts were detected on an ABI3730 automatic DNA sequencer along with GeneScan 500 LIZ size standard (Applied Biosystems). RT-PCR products were accurately sized and mean peak areas calculated using GeneMapper software.

Phylogenetic Analysis

Genes homologous to *Arabidopsis STIPL1* were identified using BLAST (Altschul et al., 1997, 2005). Protein sequences were aligned using MUSCLE (Edgar, 2004) and manually curated to remove clearly erroneous regions of alignment. A maximum likelihood phylogenetic tree was constructed using CIPRES PORTAL (Miller et al., 2010), using RAxML (Stamatakis 2006) and an "LG+I+G+F" model of protein evolution as prescribed by ProtTest (Abascal et al., 2005). Data were manipulated in JALVIEW (Waterhouse et al., 2009) and FigTree version 1.3.1.

Subcellular Localization

STIPL1-GFP imaging was completed using a Leica TCS-SP2 laser scanning spectral confocal microscope equipped with an argon ion (488 nm) excitation laser system and a ×60 objective lens. The 4′,6-diamidino-2-phenylindole fluorescence was detected following excitation at 395 nm using a UV laser. Image manipulation was completed with Leica proprietary software and ImageJ (Abramoff et al., 2004). Similar localization patterns were also observed in three independent transgenic families in which pGWB4 STIPL1 was transformed into wild-type plants.

Accession Numbers

Sequence data from this article can be found in the Arabidopsis Genome Initiative database under the following accession numbers: *CCA1*, At2g46830; *GI*, At1g22770; *LHY*, At1g01060; *PP2A*, At1g13320; *PRR9*, At2g46790; *RVE8*, At3g09600; *STIPL1*, At1g17070; *STIPL2*, At2g42330; *TOC1*, At5g61380; and *UBC21*, At5g25760. Accession numbers for plant STIP family paralogs are presented in Figure 6A. *stipl1-2* (SAIL-073187) and *stipl2-1* (GABI-425C03) seeds were obtained from the SAIL and Gabi-Kat T-DNA insertion collections, respectively (Sessions et al., 2002; Li et al., 2007).

Supplemental Data

The following materials are available in the online version of this article.

Supplemental Figure 1. Bioluminescence of *stipl1* Seedlings Containing a *CCR2:LUC* Reporter Construct.

Supplemental Figure 2. Expression of Circadian Clock–Regulated Genes in *stipl1* Seedlings under Constant Light.

Supplemental Figure 3. Investigation of Increased Bioluminescence Mutant Phenotype of *stipl1-1* Seedlings.

Supplemental Figure 4. Alternative Splicing in Selected Circadian Transcripts in *stipl* Mutants.

Supplemental Figure 5. Examination of the Abundance of Circadian Gene Alternatively Spliced Isoforms in *stipl1* Mutant Seedlings Using High-Resolution RT-PCR.

Supplemental Figure 6. Examples of Circadian Gene Alternative Splicing Events Unaffected in *stipl1* Mutant Seedlings Assessed Using High-Resolution RT-PCR.

Supplemental Figure 7. Expression of *STIPL1* and *STIPL2* over Developmental Time.

Supplemental Table 1. Gene Models Located in the *stipl1* Mapping Interval.

Supplemental References 1. References for the Supplemental Data.

Supplemental Data Set 1. Text File of the Sequences and Alignment Used for the Phylogenetic Analysis Shown in Figure 6A.

Supplemental Data Set 2. Changes in Ratios of Alternatively Spliced Products of Circadian Clock Genes in *stipl1* Alleles (Excluding Unspliced Products).

Supplemental Data Set 3. Changes in Ratios of Alternatively Spliced Products of Circadian Clock Genes in *stipl1* Alleles, Including Unspliced Products.

Supplemental Data Set 4. Changes in Ratios of Alternatively Spliced Products of Genes Not Directly Linked to the Circadian Clock in *stipl1* Alleles.

Supplemental Data Set 5. Changes in Ratios of Alternatively Spliced Products of Circadian Clock Genes in *stipl2-1* Seedlings.

Supplemental Data Set 6. Changes in Ratios of Alternatively Spliced Products of Genes Not Directly Linked to the Circadian Clock in *stipl2-1* Seedlings.

Supplemental Data Set 7. Analysis of Changes in *STIPL1* Expression in Response to Abiotic Stress.

Supplemental Data Set 8. Oligonucleotides Used for This Study.

ACKNOWLEDGMENTS

We thank Byung-kook Ham for help with confocal microscopy, Ellen Martin-Tryon for oligonucleotide sequences, Marcelo Yanovsky and Julin Maloof for helpful discussions, and Emily Buchan and Jimmy Guo for technical assistance. This work was supported by National Institutes of Health Grant GM069418 (to S.L.H.) and by grants from the Biotechnology and Biological Sciences Research Council (BB/G024979/1 European Research Area network Plant Genomics [Plant Alternative Splicing and Abiotic Stress]), the European Union FP6 Programme–European Alternative Splicing Network of Excellence (LSHG-CT-2005-518238), and the Scottish Government Rural and Environment Science and Analytical Services division (to J.W.S.B.).

AUTHOR CONTRIBUTIONS

M.A.J., J.W.S.B., and S.L.H. designed the research. M.A.J., B.A.W., and C.G.S. performed research. M.A.J., B.A.W., J.M., C.G.S., J.W.S.B., and S.L.H. analyzed data. M.A.J., J.W.S.B., and S.L.H. wrote the article.

Received September 8, 2012; revised September 8, 2012; accepted October 10, 2012; published October 30, 2012.

REFERENCES

Abascal, F., Zardoya, R., and Posada, D. (2005). ProtTest: Selection of best-fit models of protein evolution. Bioinformatics **21:** 2104–2105.

Abramoff, M.D., Magalhães, P.J., and Ram, S.J. (2004). Image processing with ImageJ. Biophotonics International **11:** 36–42.

Alabadí, D., Oyama, T., Yanovsky, M.J., Harmon, F.G., Más, P., and Kay, S.A. (2001). Reciprocal regulation between TOC1 and LHY/CCA1 within the Arabidopsis circadian clock. Science **293:** 880–883.

Alexander, R.D., Innocente, S.A., Barrass, J.D., and Beggs, J.D. (2010). Splicing-dependent RNA polymerase pausing in yeast. Mol. Cell **40:** 582–593.

Ali, G.S., and Reddy, A.S.N. (2008). Regulation of alternative splicing of pre-mRNAs by stresses. Curr. Top. Microbiol. Immunol. **326:** 257–275.

Altschul, S.F., Madden, T.L., Schäffer, A.A., Zhang, J., Zhang, Z., Miller, W., and Lipman, D.J. (1997). Gapped BLAST and PSI-BLAST: A new generation of protein database search programs. Nucleic Acids Res. **25:** 3389–3402.

Altschul, S.F., Wootton, J.C., Gertz, E.M., Agarwala, R., Morgulis, A., Schäffer, A.A., and Yu, Y.-K. (2005). Protein database searches using compositionally adjusted substitution matrices. FEBS J. **272:** 5101–5109.

Aravind, L., and Koonin, E.V. (1999). G-patch: A new conserved domain in eukaryotic RNA-processing proteins and type D retroviral polyproteins. Trends Biochem. Sci. **24:** 342–344.

Barbazuk, W.B., Fu, Y., and McGinnis, K.M. (2008). Genome-wide analyses of alternative splicing in plants: opportunities and challenges. Genome Res. **18:** 1381–1392.

Chen, M., and Manley, J.L. (2009). Mechanisms of alternative splicing regulation: Insights from molecular and genomics approaches. Nat. Rev. Mol. Cell Biol. **10:** 741–754.

Cibois, M., Gautier-Courteille, C., Legagneux, V., and Paillard, L. (2010). Post-transcriptional controls - Adding a new layer of regulation to clock gene expression. Trends Cell Biol. **20:** 533–541.

Clough, S.J., and Bent, A.F. (1998). Floral dip: A simplified method for Agrobacterium-mediated transformation of *Arabidopsis thaliana*. Plant J. **16:** 735–743.

Cokol, M., Nair, R., and Rost, B. (2000). Finding nuclear localization signals. EMBO Rep. **1:** 411–415.

Daxinger, L., Hunter, B., Sheikh, M., Jauvion, V., Gasciolli, V., Vaucheret, H., Matzke, M., and Furner, I. (2008). Unexpected silencing effects from T-DNA tags in Arabidopsis. Trends Plant Sci. **13:** 4–6.

Dodd, A.N., Salathia, N., Hall, A., Kévei, E., Tóth, R., Nagy, F., Hibberd, J.M., Millar, A.J., and Webb, A.A. (2005). Plant circadian clocks increase photosynthesis, growth, survival, and competitive advantage. Science **309:** 630–633.

Earley, K.W., Haag, J.R., Pontes, O., Opper, K., Juehne, T., Song, K., and Pikaard, C.S. (2006). Gateway-compatible vectors for plant functional genomics and proteomics. Plant J. **45:** 616–629.

Edgar, R.C. (2004). MUSCLE: Multiple sequence alignment with high accuracy and high throughput. Nucleic Acids Res. **32:** 1792–1797.

Farré, E.M., Harmer, S.L., Harmon, F.G., Yanovsky, M.J., and Kay, S.A. (2005). Overlapping and distinct roles of PRR7 and PRR9 in the Arabidopsis circadian clock. Curr. Biol. **15:** 47–54.

Farré, E.M., and Kay, S.A. (2007). PRR7 protein levels are regulated by light and the circadian clock in Arabidopsis. Plant J. **52:** 548–560.

Filichkin, S.A., and Mockler, T.C. (2012). Unproductive alternative splicing and nonsense mRNAs: a widespread phenomenon among plant circadian clock genes. Biol. Direct **7:** 20.

Filichkin, S.A., Priest, H.D., Givan, S.A., Shen, R., Bryant, D.W., Fox, S.E., Wong, W.-K., and Mockler, T.C. (2010). Genome-wide mapping of alternative splicing in *Arabidopsis thaliana*. Genome Res. **20:** 45–58.

Gendron, J.M., Pruneda-Paz, J.L., Doherty, C.J., Gross, A.M., Kang, S.E., and Kay, S.A. (2012). Arabidopsis circadian clock protein, TOC1, is a DNA-binding transcription factor. Proc. Natl. Acad. Sci. USA **109:** 3167–3172.

Harmer, S.L. (2009). The circadian system in higher plants. Annu. Rev. Plant Biol. **60:** 357–377.

Harmer, S.L., and Kreps, J. (2002). Luciferase imaging whole plants. In Arabidopsis: A Laboratory Manual, D. Weigel and J. Glazebrook, eds (Cold Spring Harbor, NY: Cold Spring Harbor Laboratory Press), pp. 269–279.

Hong, S., Song, H.-R., Lutz, K., Kerstetter, R.A., Michael, T.P., and McClung, C.R. (2010). Type II protein arginine methyltransferase 5 (PRMT5) is required for circadian period determination in *Arabidopsis thaliana*. Proc. Natl. Acad. Sci. USA **107:** 21211–21216.

Huang, W., Pérez-García, P., Pokhilko, A., Millar, A.J., Antoshechkin, I., Riechmann, J.L., and Mas, P. (2012). Mapping the core of the Arabidopsis circadian clock defines the network structure of the oscillator. Science **336:** 75–79.

Huang, Y., Genova, G., Roberts, M., and Jackson, F.R. (2007). The LARK RNA-binding protein selectively regulates the circadian eclosion rhythm by controlling E74 protein expression. PLoS ONE **2:** e1107.

Hut, R.A., and Beersma, D.G.M. (2011). Evolution of time-keeping mechanisms: Early emergence and adaptation to photoperiod. Philos. Trans. R. Soc. Lond. B Biol. Sci. **366:** 2141–2154.

Iliev, D., Voytsekh, O., Schmidt, E.-M., Fiedler, M., Nykytenko, A., and Mittag, M. (2006). A heteromeric RNA-binding protein is involved in maintaining acrophase and period of the circadian clock. Plant Physiol. **142:** 797–806.

James, A.B., Syed, N.H., Bordage, S., Marshall, J., Nimmo, G.A., Jenkins, G.I., Herzyk, P., Brown, J.W.S., and Nimmo, H.G. (2012). Alternative splicing mediates responses of the *Arabidopsis* circadian clock to temperature changes. Plant Cell **24:** 961–981.

Jander, G., Norris, S.R., Rounsley, S.D., Bush, D.F., Levin, I.M., and Last, R.L. (2002). Arabidopsis map-based cloning in the post-genome era. Plant Physiol. **129:** 440–450.

Ji, Q., Huang, C.-H., Peng, J., Hashmi, S., Ye, T., and Chen, Y. (2007). Characterization of STIP, a multi-domain nuclear protein, highly conserved in metazoans, and essential for embryogenesis in *Caenorhabditis elegans*. Exp. Cell Res. **313:** 1460–1472.

Jones, M.A. (2009). Entrainment of the Arabidopsis circadian clock. J. Plant Biol. **52:** 202–209.

Jones, M.A., Covington, M.F., DiTacchio, L., Vollmers, C., Panda, S., and Harmer, S.L. (2010). Jumonji domain protein JMJD5 functions in both the plant and human circadian systems. Proc. Natl. Acad. Sci. USA **107:** 21623–21628.

Jurica, M.S., Licklider, L.J., Gygi, S.R., Grigorieff, N., and Moore, M.J. (2002). Purification and characterization of native spliceosomes suitable for three-dimensional structural analysis. RNA **8:** 426–439.

Kalyna, M., et al. (2012). Alternative splicing and nonsense-mediated decay modulate expression of important regulatory genes in Arabidopsis. Nucleic Acids Res. **40:** 2454–2469.

Kilian, J., Whitehead, D., Horak, J., Wanke, D., Weinl, S., Batistic, O., D'Angelo, C., Bornberg-Bauer, E., Kudla, J., and Harter, K. (2007). The AtGenExpress global stress expression data set: protocols, evaluation and model data analysis of UV-B light, drought and cold stress responses. Plant J. **50:** 347–363.

Kim, W.Y., Fujiwara, S., Suh, S.S., Kim, J., Kim, Y., Han, L., David, K., Putterill, J., Nam, H.G., and Somers, D.E. (2007). ZEITLUPE is a circadian photoreceptor stabilized by GIGANTEA in blue light. Nature **449:** 356–360.

Kojima, S., Shingle, D.L., and Green, C.B. (2011). Post-transcriptional control of circadian rhythms. J. Cell Sci. **124:** 311–320.

Li, Y., Rosso, M.G., Viehoever, P., and Weisshaar, B. (2007). GABI-Kat SimpleSearch: An *Arabidopsis thaliana* T-DNA mutant database with detailed information for confirmed insertions. Nucleic Acids Res. **35**(Database issue)**:** D874–D878.

Luco, R.F., and Misteli, T. (2011). More than a splicing code: integrating the role of RNA, chromatin and non-coding RNA in alternative splicing regulation. Curr. Opin. Genet. Dev. **21:** 366–372.

Luco, R.F., Pan, Q., Tominaga, K., Blencowe, B.J., Pereira-Smith, O.M., and Misteli, T. (2010). Regulation of alternative splicing by histone modifications. Science **327:** 996–1000.

Lukowitz, W., Gillmor, C.S., and Scheible, W.R. (2000). Positional cloning in Arabidopsis. Why it feels good to have a genome initiative working for you. Plant Physiol. **123:** 795–805.

Makarov, E.M., Makarova, O.V., Urlaub, H., Gentzel, M., Will, C.L., Wilm, M., and Lührmann, R. (2002). Small nuclear ribonucleoprotein remodeling during catalytic activation of the spliceosome. Science **298:** 2205–2208.

Marquez, Y., Brown, J.W.S., Simpson, C., Barta, A., and Kalyna, M. (2012). Transcriptome survey reveals increased complexity of the alternative splicing landscape in Arabidopsis. Genome Res. **22:** 1184–1195.

Martin-Tryon, E.L., Kreps, J.A., and Harmer, S.L. (2007). GIGANTEA acts in blue light signaling and has biochemically separable roles in circadian clock and flowering time regulation. Plant Physiol. **143:** 473–486.

Más, P., Kim, W.-Y., Somers, D.E., and Kay, S.A. (2003). Targeted degradation of TOC1 by ZTL modulates circadian function in *Arabidopsis thaliana*. Nature **426:** 567–570.

McCracken, S., Fong, N., Yankulov, K., Ballantyne, S., Pan, G., Greenblatt, J., Patterson, S.D., Wickens, M., and Bentley, D.L. (1997). The C-terminal domain of RNA polymerase II couples mRNA processing to transcription. Nature **385:** 357–361.

Miller, M.A., Pfeiffer, W., and Schwartz, T. (2010). Creating the CIPRES Science Gateway for inference of large phylogenetic trees. Gateway Computing Environments Workshop, pp. 1–8.

Nakagawa, T., Kurose, T., Hino, T., Tanaka, K., Kawamukai, M., Niwa, Y., Toyooka, K., Matsuoka, K., Jinbo, T., and Kimura, T. (2007). Development of series of gateway binary vectors, pGWBs, for realizing efficient construction of fusion genes for plant transformation. J. Biosci. Bioeng. **104:** 34–41.

Nakahata, Y., Kaluzova, M., Grimaldi, B., Sahar, S., Hirayama, J., Chen, D., Guarente, L.P., and Sassone-Corsi, P. (2008). The NAD+-dependent deacetylase SIRT1 modulates CLOCK-mediated chromatin remodeling and circadian control. Cell **134:** 329–340.

Nakamichi, N. (2011). Molecular mechanisms underlying the Arabidopsis circadian clock. Plant Cell Physiol. **52:** 1709–1718.

Nakamichi, N., Kiba, T., Henriques, R., Mizuno, T., Chua, N.-H., and Sakakibara, H. (2010). PSEUDO-RESPONSE REGULATORS 9, 7, and 5 are transcriptional repressors in the *Arabidopsis* circadian clock. Plant Cell **22:** 594–605.

Paine, C.T., Paine, M.L., Luo, W., Okamoto, C.T., Lyngstadaas, S.P., and Snead, M.L. (2000). A tuftelin-interacting protein (TIP39) localizes to the apical secretory pole of mouse ameloblasts. J. Biol. Chem. **275:** 22284–22292.

Panda, S., Poirier, G.G., and Kay, S.A. (2002). tej defines a role for poly(ADP-ribosyl)ation in establishing period length of the arabidopsis circadian oscillator. Dev. Cell **3:** 51–61.

Plautz, J.D., Straume, M., Stanewsky, R., Jamison, C.F., Brandes, C., Dowse, H.B., Hall, J.C., and Kay, S.A. (1997). Quantitative

analysis of Drosophila period gene transcription in living animals. J. Biol. Rhythms **12:** 204–217.

Rappsilber, J., Ryder, U., Lamond, A.I., and Mann, M. (2002). Large-scale proteomic analysis of the human spliceosome. Genome Res. **12:** 1231–1245.

Rosbash, M. (2009). The implications of multiple circadian clock origins. PLoS Biol. **7:** e62.

Rost, F.W.D. (1995). Fluorescence Microscopy. (Cambridge, UK: Cambridge University Press).

Sanchez, S.E., et al. (2010). A methyl transferase links the circadian clock to the regulation of alternative splicing. Nature **468:** 112–116.

Seo, P.J., Park, M.-J., Lim, M.-H., Kim, S.-G., Lee, M., Baldwin, I.T., and Park, C.-M. (2012). A self-regulatory circuit of CIRCADIAN CLOCK-ASSOCIATED1 underlies the circadian clock regulation of temperature responses in *Arabidopsis*. Plant Cell **24:** 2427–2442.

Sessions, A., et al. (2002). A high-throughput *Arabidopsis* reverse genetics system. Plant Cell **14:** 2985–2994.

Simpson, C.G., Fuller, J., Maronova, M., Kalyna, M., Davidson, D., McNicol, J., Barta, A., and Brown, J.W.S. (2008). Monitoring changes in alternative precursor messenger RNA splicing in multiple gene transcripts. Plant J. **53:** 1035–1048.

Staiger, D., and Green, R. (2011). RNA-based regulation in the plant circadian clock. Trends Plant Sci. **16:** 517–523.

Staley, J.P., and Guthrie, C. (1998). Mechanical devices of the spliceosome: Motors, clocks, springs, and things. Cell **92:** 315–326.

Stamatakis, A. (2006). RAxML-VI-HPC: Maximum likelihood-based phylogenetic analyses with thousands of taxa and mixed models. Bioinformatics **22:** 2688–2690.

Strayer, C., Oyama, T., Schultz, T.F., Raman, R., Somers, D.E., Más, P., Panda, S., Kreps, J.A., and Kay, S.A. (2000). Cloning of the Arabidopsis clock gene TOC1, an autoregulatory response regulator homolog. Science **289:** 768–771.

Svec, M., Bauerová, H., Pichová, I., Konvalinka, J., and Strísovský, K. (2004). Proteinases of betaretroviruses bind single-stranded nucleic acids through a novel interaction module, the G-patch. FEBS Lett. **576:** 271–276.

Tannukit, S., Crabb, T.L., Hertel, K.J., Wen, X., Jans, D.A., and Paine, M.L. (2009). Identification of a novel nuclear localization signal and speckle-targeting sequence of tuftelin-interacting protein 11, a splicing factor involved in spliceosome disassembly. Biochem. Biophys. Res. Commun. **390:** 1044–1050.

van Ooijen, G., Dixon, L.E., Troein, C., and Millar, A.J. (2011). Proteasome function is required for biological timing throughout the twenty-four hour cycle. Curr. Biol. **21:** 869–875.

Wang, B.-B., and Brendel, V. (2004). The ASRG database: Identification and survey of *Arabidopsis thaliana* genes involved in pre-mRNA splicing. Genome Biol. **5:** R102.

Wang, X., et al. (2012). SKIP is a component of the spliceosome linking alternative splicing and the circadian clock in *Arabidopsis*. Plant Cell **24:** 3278–3295.

Waterhouse, A.M., Procter, J.B., Martin, D.M.A., Clamp, M., and Barton, G.J. (2009). Jalview Version 2—A multiple sequence alignment editor and analysis workbench. Bioinformatics **25:** 1189–1191.

Will, C.L., and Lührmann, R. (2011). Spliceosome structure and function. Cold Spring Harb. Perspect. Biol. **3:** a003707.

Zhang, L., Weng, W., and Guo, J. (2011). Posttranscriptional mechanisms in controlling eukaryotic circadian rhythms. FEBS Lett. **585:** 1400–1405.

Zhou, Z., Licklider, L.J., Gygi, S.P., and Reed, R. (2002). Comprehensive proteomic analysis of the human spliceosome. Nature **419:** 182–185.

Mutation of *Arabidopsis SPLICEOSOMAL TIMEKEEPER LOCUS1* Causes Circadian Clock Defects

Matthew A. Jones, Brian A. Williams, Jim McNicol, Craig G. Simpson, John W.S. Brown and Stacey L. Harmer

Plant Cell; originally published online October 30, 2012;
DOI 10.1105/tpc.112.104828